Handling geological and economic uncertainties in balancing short-term and long-term objectives in waterflooding optimization

Siraj, Mohsin; van den Hof, Paul; Jansen, Jan Dirk

DOI
10.2118/185954-PA

Publication date
2017

Document Version
Final published version

Published in
SPE Journal

Handling Geological and Economic Uncertainties in Balancing Short-Term and Long-Term Objectives in Waterflooding Optimization

M. Mohsin Siraj and **Paul M. J. Van den Hof,** Eindhoven University of Technology, and
Jan-Dirk Jansen, Delft University of Technology

Summary

Model-based economic optimization of oil production has a significant scope to increase financial life-cycle performance. The net-present-value (NPV) objective in this optimization, because of its nature, focuses on long-term gains, whereas short-term production is not explicitly addressed. At the same time, the achievable NPV is highly uncertain because of strongly varying economic conditions and limited knowledge of the reservoir-model parameters. The prime focus of this work is to develop optimization strategies that balance both long-term and short-term economic objectives and also offer robustness to the long-term NPV. An earlier robust hierarchical optimization method honoring geological uncertainty with robust long-term and short-term NPV objectives serves as a starting base of this work. We address the issue of extending this approach to include economic uncertainty and aim to analyze how the optimal solution reduces the uncertainty in the achieved average NPV. An ensemble of varying oil prices is used to model economic uncertainty with average NPVs as robust objectives in the hierarchical approach. A weighted-sum approach is used with the same objectives to quantify the effect of uncertainty. To reduce uncertainty, a mean-variance-optimization (MVO) objective is then considered to maximize the mean and also minimize the variance. A reduced effect of uncertainty on the long-term NPV is obtained compared with the uncertainty in the mean-optimization (MO) objectives. Last, it is investigated whether, because of the better handling of uncertainty in MVO, a balance between short-term and long-term gains can be naturally obtained by solving a single-objective MVO. Simulation examples show that a faster NPV buildup is naturally achieved by choosing appropriate weighting of the variance term in the MVO objective.

Introduction

Dynamic optimization of waterflooding has shown significant scope for improvement of the economic life-cycle performance of oil fields compared with a conventional reactive strategy (Brouwer and Jansen 2004; Sarma et al. 2005; Jansen et al. 2008; Chen and Oliver 2010; Chen et al. 2010; Foss 2012; Van den Hof et al. 2012). In these studies, the financial measure NPV is maximized.

NPV is defined as the cumulative discounted cash flow (CDCF) over the production life cycle of the reservoir. Here, we only consider contributions to the NPV originating from the injection and production of fluids, whereas other contributions, such as capital expenditures, do not play a role in the optimization formulation. The optimization problem considered in the publications mentioned previously focuses on long-term gains, whereas short-term production is generally neglected. This typically results in low short-term gains compared with those resulting from a reactive strategy. Furthermore, because of the high levels of uncertainty in this model-based economic optimization, the resulting optimal strategy is highly uncertain. This uncertainty mainly arises from strongly varying economic conditions and from geological uncertainties in the modeling process of waterflooding.

As a result, the potential advantages of such optimization are not fully realized and the risk of not reaching the predicted NPV becomes very high. High short-term gains are often important to maximize cash flow or meet short-term goals such as production contracts. An (ad hoc) way to increase the momentary rate of oil production, and hence the short-term gains while maintaining a long-term objective, has been proposed in van Essen et al. (2011), who used a lexicographic or hierarchical multiobjective-optimization approach. NPV with a high discount factor has been maximized as a secondary objective to improve short-term gains under the condition that the primary objective (i.e., an undiscounted NPV) stays close to its optimal value. Chen et al. (2012) added robustness while balancing both objectives through solving a robust optimization problem under geological uncertainty. An average short-term NPV over an ensemble of reservoir models has been maximized while explicitly enforcing, by use of an augmented Langrangian method, the optimality condition of the average long-term NPV as a constraint. The average objectives have been inspired by van Essen et al. (2009). In Chen et al. (2012) and Fonseca et al. (2014), the hierarchical approach of van Essen et al. (2011) has been extended in a similar fashion but by use of a different optimization method.

The main focus of this work is to devise optimal solutions to the life-cycle-optimization problem that balance short-term and long-term gains, and at the same time provide robustness to the predicted NPV under both economic and geological uncertainty. Starting with a base example from the work of van Essen et al. (2011) and Fonseca et al. (2014), we address this question: Can a similar robust framework with primary (long-term) and secondary (short-term) objectives be formulated under economic uncertainty? And, more importantly, do these robust multiobjective-optimization (MOO) formulations provide better uncertainty handling? An ensemble of varying oil prices is considered to model economic uncertainty, and an average of long-term and short-term NPV over the ensemble is optimized by use of the hierarchical approach. A redundant degrees-of-freedom (DOFs) analysis for the robust long-term NPV solution is explicitly performed and it is shown that the solution is nonunique, allowing a short-term objective to be optimized, as in Siraj et al. (2015b).

To answer the question of uncertainty handling of MOO, a more-generic weighted-sum MOO approach with the same objectives is used to characterize and quantify the effect of the uncertainty on the objective functions. With varying weights, it leads to a so-called robust Pareto curve, which quantitatively gives the bounds of the effect of uncertainty on the primary- and secondary-objective functions. The definition or selection of the robust objectives in MOO is an important consideration because it defines how the uncertainty is treated in an optimization problem. These average or MO objectives are classified as risk-neutral approaches (Rockafellar 2007). MO includes uncertainty in the optimization framework, but the optimized solution does not lead

Original SPE manuscript received for review 11 July 2016. Revised manuscript received for review 1 December 2016. Paper (SPE 185954) peer approved 19 January 2017.

to a reduced uncertainty in the achieved NPV. For better uncertainty handling of these MOOs, we are inspired by the seminal work of "risk-return" portfolio management (Markowitz 1952), which has been applied to robust waterflooding optimization under geological uncertainty by Capolei et al. (2015b), to consider a risk-averse MVO objective. In MVO, the risk is quantified by the variance of the NPV distribution. MVO with maximization of the average NPV minimizes the variance of the NPV distribution. The robust weighted-sum approach is then used with long-term and short-term MVO objectives. The proposed approach provides a more-robust solution for the long-term NPV compared with the MO approach. Note that these robust MOO approaches can easily be extended to consider other risk-averse objectives, such as mean-conditional value at risk and mean-worst case (Rockafellar 2007; Capolei et al. 2015a; Liu and Reynolds 2015a; Siraj et al. 2015c).

By changing the NPV objective, these optimization methods provide an indirect or ad hoc way of balancing the short-term and the long-term economic objectives. In Capolei et al. (2015b), a bicriterion MVO function has been optimized and key economic indicators have been given. We consider a single-objective MVO to investigate whether, by explicit handling of uncertainty in model-based economic optimization, the balance between short-term and long-term gains can be naturally obtained. This essentially means moving from MOO to a single-objective MVO to study the relationship between uncertainty handling and obtaining a natural balance between short-term and long-term gains. MVO is implemented and also extended to explicitly consider economic uncertainty. Similar MVO approaches have been described in Siraj et al. (2015a), and for a well-placement problem in Yeten et al. (2003).

Robust Optimization in Waterflooding

Waterflooding. In waterflooding, water is injected to maintain reservoir pressure and displace oil toward the producing wells. The dynamics of the waterflooding process can be described by conservation-of-mass and-momentum equations (Darcy's law) (Aziz and Settari 1979; Jansen et al. 2008). A state/space form results after discretization of the governing equations in both space and time:

$$\mathbf{g}_k(\mathbf{u}_k, \mathbf{x}_k, \mathbf{x}_{k-1}, \boldsymbol{\theta}) = \mathbf{0}, \quad k = 1, \ldots, K, \quad \ldots\ldots\ldots\ldots (1)$$

$$\mathbf{y}_k = \mathbf{h}_k(\mathbf{u}_k, \mathbf{x}_k), \quad \ldots\ldots\ldots\ldots\ldots\ldots\ldots\ldots (2)$$

where subscripts refer to discrete instants k of time; K is the total number of timesteps; and $\mathbf{g}$ and $\mathbf{h}$ are nonlinear vector-valued functions. In reservoir simulation of waterflooding, the state variables, which form the elements of vector $\mathbf{x}_k \in N \subset \mathbb{R}^n$, are typically pressures and water saturations in each grid cell with initial conditions $\mathbf{x}_0 = \overline{\mathbf{x}}_0$. Note that $\mathbf{x}_k$ is a shortcut notation to represent $\mathbf{x}_k = \mathbf{x}(t_k)$; i.e., the value of $\mathbf{x}$ at time $t = t_k$. The control vector $\mathbf{u}_k \in M \subset \mathbb{R}^m$ can represent a combination of prescribed well-flow rates, wellbore pressures, or valve settings. The parameter vector $\boldsymbol{\theta} \in \Theta \subset \mathbb{R}^{n_\theta}$ typically contains porosities and permeabilities in each grid cell, and other uncertain parameters such as fault-transmissibility multipliers and initial fluid contacts. Measured output variables are denoted by $\mathbf{y}_k$.

For a given well configuration, the injection-flow rates and/or production-valve settings can be dynamically operated over the production life cycle, and therefore serve as control inputs for optimization. The objective is to maximize a financial measure, NPV, over a fixed time horizon, which can be represented in the usual fashion as

$$J = \sum_{k=1}^{K} \left[\frac{r_o \cdot q_{o,k} - r_w \cdot q_{w,k} - r_{\text{inj}} \cdot q_{\text{inj},k}}{(1+b)^{\frac{t_k}{\tau_t}}} \cdot \Delta t_k \right], \quad \ldots\ldots (3)$$

where r_o, r_w, and r_{inj} are the oil price, the water-production cost, and the water-injection cost in USD/m^3, respectively, and Δt_k is the time interval of timestep k in days. The term b is the discount rate for a certain reference time τ_t. The terms $q_{o,k}, q_{w,k}$, and $q_{\text{inj},k}$ represent the total flow rate of produced oil, produced water, and injected water at timestep k in m^3/d.

In this work, a gradient-based optimization approach is used in which the gradients are obtained by solving a system of adjoint equations (Sarma et al. 2005; Jansen 2011).

Robust Hierarchical Optimization. In Haimes and Li (1988), a hierarchical or lexicographic method has been described allowing prioritization of multiple objectives. In van Essen et al. (2011), this hierarchical approach has been used to balance long-term and short-term gains by distinguishing the long-term NPV (J_1) and a secondary (short-term) objective with highly discounted NPV (J_2). The optimization of the secondary objective is constrained by the condition that the primary (long-term) objective should remain close to its optimal value J_1^*. It can be formulated as

$$\begin{aligned} &\max_{\mathbf{u}_{1:K}} J_2 \\ &\text{subject to (s.t.) } \mathbf{g}_k(\mathbf{u}_k, \mathbf{x}_k, \mathbf{x}_{k-1}, \boldsymbol{\theta}) = \mathbf{0}, \ \ \mathbf{y}_k = \mathbf{h}(\mathbf{u}_k, \mathbf{x}_k), \ \ \mathbf{x}_0 = \overline{\mathbf{x}}_0, \\ &\mathbf{c}(\mathbf{u}_k, \mathbf{y}_k) = \mathbf{0}, \ \ \mathbf{d}(\mathbf{u}_k, \mathbf{y}_k) \le \mathbf{0}, \\ &J_1^* - J_1 \le \varepsilon, \qquad \ldots\ldots\ldots\ldots\ldots\ldots\ldots\ldots (4) \end{aligned}$$

where $\mathbf{c}(\mathbf{u}_k, \mathbf{y}_k)$ and $\mathbf{d}(\mathbf{u}_k, \mathbf{y}_k)$ are equality and inequality constraints, respectively, and where the notation $1:K$ indicates the set of timesteps $k = 1, 2, \ldots, K$, which spans the entire production life cycle. In van Essen et al. (2011), it has been shown that this procedure can lead to substantially higher revenues in the short term, with only very-minor compromises for the long-term gains. This potential to increase the short-term gains originates from the fact that the original long-term optimization problem (Eq. 4) has redundant DOFs.

In Fonseca et al. (2014), this hierarchical approach has been extended to a robust setting, taking account of geological-model uncertainty according to the robust optimization formulation of van Essen et al. (2009). In van Essen et al. (2009), an ensemble of possible geological realizations is used to determine an average NPV over that set, leading to the MO approach, determined by the objective function:

$$J_{MO} = \frac{1}{N_{\text{geo}}} \sum_{i=1}^{N_{\text{geo}}} J^i, \quad \ldots\ldots\ldots\ldots\ldots\ldots (5)$$

where N_{geo} is the number of realizations. This same principle can now be used in the hierarchical setting by considering the long-term mean revenue $J_{MO,1}$ and the short-term mean revenue $J_{MO,2}$, defined in accordance with Eq. 5.

Base-Case Example

The simulation example that we consider as a base case is the same as the one presented in van Essen et al. (2009) (in the nominal case) and Fonseca et al. (2014). We have used an ensemble of 100 geological realizations of the standard egg model, which is publicly available (Jansen et al. 2014). Each model is a 3D realization of a channelized reservoir produced under waterflooding conditions with eight water injectors and four producers. The production life cycle of each reservoir model is 3,600 days. The absolute permeability field of the first realization in the set is shown in **Fig. 1.** For all other reservoir and fluid parameters, we refer to Jansen et al. (2014). All the simulation experiments in this work are performed by use of the Matlab Reservoir Simulation Toolbox (Lie et al. 2012). All economic parameters are considered as fixed. For the primary objective, an undiscounted NPV is used. Other economic parameters, such as oil price r_o, water injection r_{inj}, and production cost r_w, are chosen as USD 126, USD 6, and USD 19/m^3, respectively. We note that the oil price is much lower than the typical present-day value. However, we have chosen to use the same value as applied by van Essen et al. (2009) to allow for a comparison of results.

The control input $\mathbf{u}_k$ involves injection-flow-rate trajectories for each of the eight injection wells. The minimum and the maximum rate for each injection well are set as 0.2 and 79.5 m^3/d,

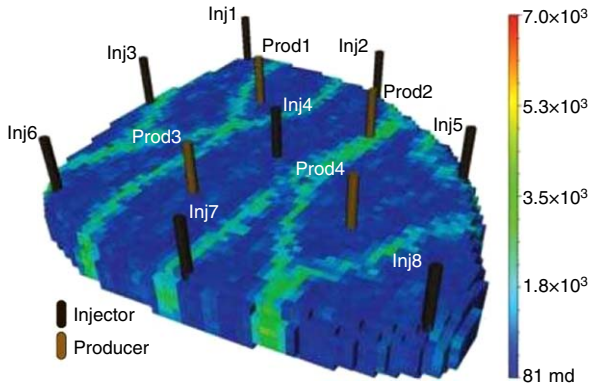

Fig. 1—Permeability field of Realization 1 of a set of 100 realizations.

respectively. The production wells operate at a constant bottomhole pressure of 395 bar. The set of control inputs $\mathbf{u}_{1:K}$ is reparameterized in control-time intervals with input parameter vector $\boldsymbol{\varphi}$. For each of the eight injection wells, the control inputs $\mathbf{u}_{1:K}$ are reparameterized into 10 time periods of t_φ of 360 days, during which the injection rate is held constant at value φ_i. Thus, the input parameter vector $\boldsymbol{\varphi}$ consists of $N_u = 8 \times 10 = 80$ elements.

As an optimization procedure to solve for the robust version of the problem (Eq. 4), a switching method is applied, as presented in van Essen et al. (2011), whereas ε is chosen at a level of 0.3% from the optimal value of the primary objective function $J_{MO,1}$. The obtained optimal inputs are applied to each member of the ensemble and the corresponding distribution of the resulting NPVs is shown in **Fig. 2a,** indicated as "robust hierarchical." This distribution is compared with the distribution resulting from applying the optimal inputs resulting from MO of $J_{MO,1}$ only, and with a reactive-control (RC) strategy applied to each ensemble member. It can be observed that because of the availability of redundant DOFs, the primary long-term objective is almost the same as with the robust hierarchical optimization.

The time evolutions of the NPV for all three strategies are compared in Fig. 2b. We note that NPV is often defined as the CDCF over the entire project life. Here we have chosen to use the term NPV also for intermediate values of the CDCF. The maximum and minimum values of the time evolutions of NPV form a band. The width of the band shows the variability of a strategy over the ensemble of the model realizations. Because the secondary objective is aimed at maximizing the oil-production rate, the short-term gains are heavily weighted, which can be observed in Fig. 2. These improved short-term gains are achieved with approximately no compromise to the long-term NPV. Hence, for this example, the robust hierarchical approach provides a good balance between long-term and short-term objectives. The reactive strategy leads to high short-term gains but at the cost of compromising long-term revenues.

For comparison with the nonhierarchical approach, the results are compared with a nominal and robust optimization of the long-term gains $J_{MO,1}$ only. In nominal optimization (NO), a single realization of the standard egg model is used for optimization. The optimization is repeated for each ensemble member, resulting in 100 NO strategies. A different number of control timesteps (20) is used because the optimization runs into numerical problems with 10 control steps. Thus, in this case, the input parameter vector $\boldsymbol{\varphi}$ consists of $N_u = 8 \times 20 = 160$ elements. The results are displayed in **Fig. 3.** Fig. 3a, which is similar to the one shown in van Essen et al. (2009), shows the probability-density function (PDF) of NPV resulting from 100 NOs, robust MO, and RC strategies (optimal inputs applied to all 100 ensemble members). It shows that MO, on average, performs better than all NO strategies, but the key point to note is that it does not aim to minimize the effect of uncertainty, such as by reducing the variance of NPV distribution. The effect of uncertainty on the time evolutions of NPV is shown in Fig. 3b. Each NO strategy is applied to the respective model that is used for optimization, whereas optimal inputs from MO and RC are applied to all ensemble members. It can also be observed that the short-term gains of the MO approach are very low compared with those of the RC approach.

The advantages of the hierarchical approach, also in its robust form, suggest that the corresponding robust optimization problem has redundant DOFs. This is illustrated by evaluating the singular-value decomposition of the (approximate) Hessian. Unfortunately, no reservoir simulator is currently equipped to compute second-order derivatives. However, there are different approximation methods available in the literature to approximate the Hessian matrix (Nocedal and Wright 2006). A forward-difference scheme to the approximate Hessian matrix, **H,** is used with the primary objective $J_{MO,1}$. Its elements H_{ij} can be expressed as

$$H_{ij} = \frac{\partial^2 J_{MO,1}}{\partial u_i \partial u_j} \approx \frac{\nabla J_{MO,1i}(\mathbf{u}_k + h_j \mathbf{e}_j) - \nabla J_{MO,1i}(\mathbf{u}_k)}{2h_j} + \frac{\nabla J_{MO,1j}(\mathbf{u}_k + h_i \mathbf{e}_i) - \nabla J_{MO,1j}(\mathbf{u}_k)}{2h_i}, \quad \cdots\cdots\cdots (6)$$

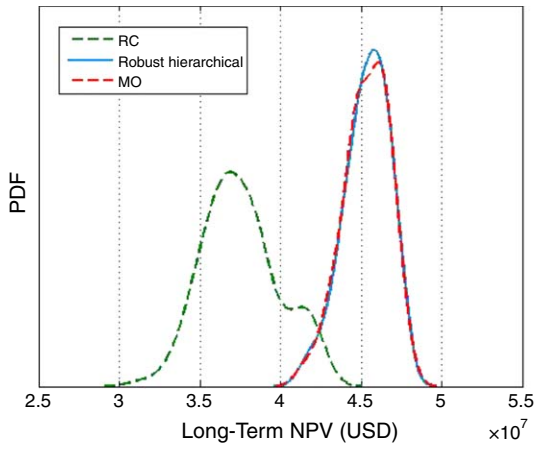

(a) PDF (long-term NPV) by applying optimal inputs from MO, robust hierarchical, and RC to each ensemble member

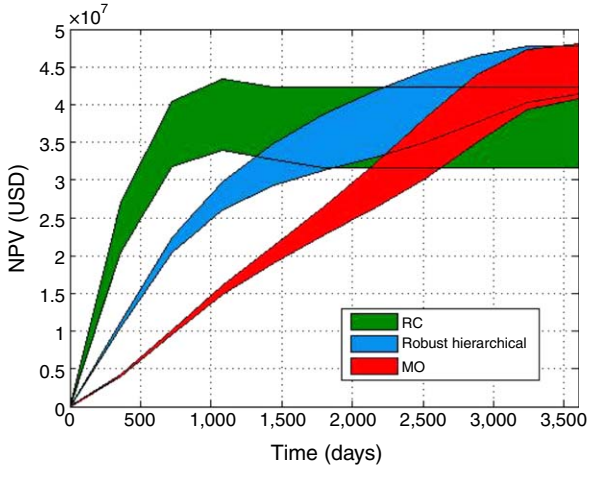

(b) Maximum and minimum (band) for time evolutions of NPV by applying optimal inputs from MO, robust hierarchical, and RC to each ensemble member

Fig. 2—Results comparison in terms of long-term and time evolutions of NPV for MO and robust hierarchical optimization under geological uncertainty with RC.

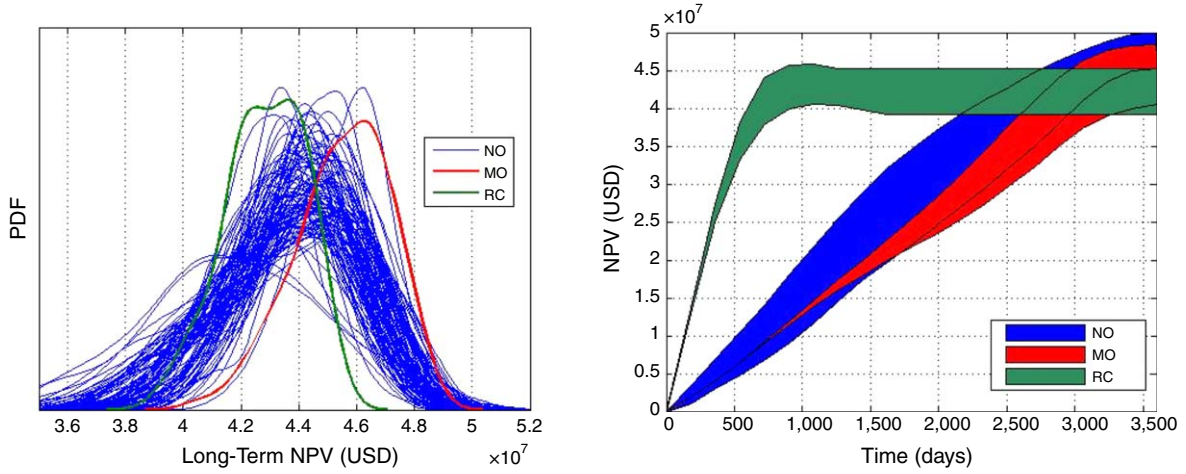

(a) PDF (long-term NPV) by applying optimal inputs from NO, RC, and MO to each ensemble member

(b) Maximum and minimum (band) for time evolutions of NPV by applying optimal inputs from MO and RC to each ensemble member while NO is applied to respective model used for optimization

Fig. 3—Results comparison in terms of long-term and time evolutions of NPV for MO under geological uncertainty with NO and RC.

where $\nabla J_{MO,1i}$ is the ith element of the gradient $\nabla J_{MO,1} = \left(\frac{\partial J_{MO,1}}{\partial \mathbf{u}}\right)^{\top}$, $\mathbf{e}_i$ is a canonical-unit vector (i.e., a vector with unity at element i and zero elsewhere), and h_i is the perturbation-step size. In total, $N_u + 1$ simulations (function evaluations) are required to obtain the approximate Hessian at a particular optimal solution $\mathbf{u}^*$, where N_u is the number of input elements. If the Hessian is negative semidefinite, it does not have full rank. The zero singular values $\sigma_i = 0$ in a singular value decomposition of $\mathbf{H}$ are given as

$$\mathbf{H} = \mathbf{U}\boldsymbol{\Sigma}\mathbf{V}^{\top}, \quad \ldots\ldots\ldots\ldots\ldots\ldots\ldots\ldots\ldots\ldots (7)$$

which determines the nonuniqueness of the solution. $\mathbf{U}$ and $\mathbf{V}$ are matrices with orthogonal columns (Strang 2011). The resulting singular values of this Hessian for the robust optimization objective $J_{MO,1}$ are shown in **Fig. 4.** By use of a threshold level through which singular values σ_i are considered to be zero when $\sigma_i/\sigma_1 < 0.02$, where σ_1 is the first and largest singular value, it appears that in the optimized input 121 DOFs are redundant. This freedom is used in the hierarchical approach to improve the short-term revenues without heavily compromising the optimality of the considered robust primary objective.

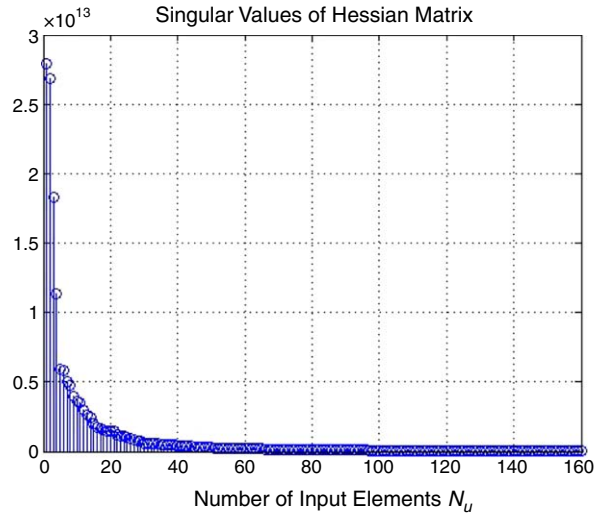

Fig. 4—Singular values of Hessian with primary objective $J_{MO,1}$ under geological uncertainty.

Robust Hierarchical Optimization Under Economic Uncertainty

The NPV objective function contains economic variables such as interest rate and oil price that fluctuate with time and cannot be precisely predicted. The unknown time variation of these variables becomes another major source of uncertainty. Among other uncertain economic variables in NPV, varying oil prices have the most dominant effect. Hence, the unknown time variation of the oil price is considered as the prime source of economic uncertainty.

Reservoir Models and Economic Data for NPV. Because the purpose of this simulation example is to show the effect of economic uncertainty on the optimal strategy, a single model realization of the standard egg model, as shown in Fig. 1, is used.

As the primary objective, an undiscounted NPV is used. Other economic parameters—such as water-injection cost r_{inj} and production cost r_w—are kept fixed at USD 23 and USD 71/m^3, respectively. There are various ways to predict the future values of changing oil prices. Different models, such as the Prospective Outlook on Long-Term Energy Systems (POLES) used by the EU and the French government and the National Energy Modeling System (NEMS) of US energy markets created at the US Department of Energy and the Energy Information Administration, are used for energy-price prediction (Criqui 2001; Lapillonne et al. 2007; Bhattacharyya and Timilsina 2010; Birol 2010). However, for this example, a simplified auto-regressive-moving-average model (Ljung 1999) is used to generate an oil-price time series. The auto-regressive-moving-average model is given by

$$r_{o_k} = a_0 + \sum_{i=1}^{6} a_i r_{o_{k-i}}, \quad \ldots\ldots\ldots\ldots\ldots\ldots\ldots\ldots (8)$$

where a_i are randomly selected coefficients. A total of 10 scenarios (i.e., $N_{\text{eco}} = 10$) with a base oil price of USD 471/m^3 are generated as shown in **Fig. 5.**

Control Input and Control Strategies. The control input and the bounds on these inputs are the same as used in the previous examples, but for this case, the control input $\mathbf{u}_{1:K}$ is reparameterized into 10 time periods of $t_\varphi = 360$ days, during which the

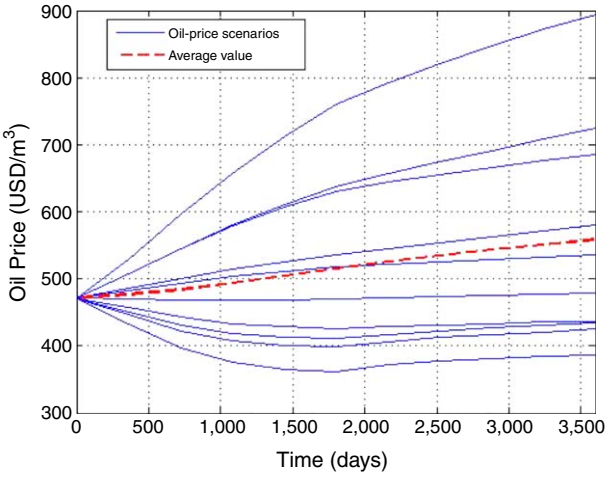

Fig. 5—Oil price according to scenarios for economic-uncertainty characterization.

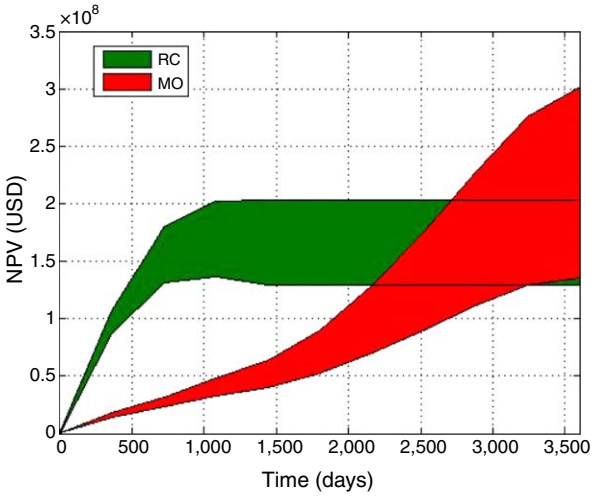

Fig. 6—Time evolutions of NPV by applying optimal inputs from MO ($J_{MO,1}$) under economic uncertainty and RC to each ensemble member.

injection rate is held constant at a value of φ_i. Thus, the input parameter vector $\boldsymbol{\varphi}$ consists of $N_u = 8 \times 10 = 80$ elements. The MO and the RC strategies are also considered.

Results for the Primary Objective. The $J_{MO,1}$ for the case of economic uncertainty is optimized by use of a gradient-based line-search-optimization procedure. The MO objective J_{MO} is as defined in Eq. 5 except that in this case of economic uncertainty, the average is taken over the oil-price scenarios for a single reservoir model. Therefore, only one uncertainty is considered at a time. The optimal strategy is applied to the reservoir model with all oil-price realizations. RC is also used. The time evolutions of NPV for both strategies are compared in **Fig. 6.** The maximum and the minimum values of the time evolutions of NPV will form a band. The first observation is the large width of these bands, which reflects a dominant effect of economic uncertainty on the strategies. MO provides a higher long-term average NPV compared with RC and performs better than RC. Intuitively, optimization should lead to increased oil production when the oil prices are higher, and vice versa. Because the mean oil price, as shown in Fig. 5, tends to increase over time, MO delays the production until the end phase of the life cycle. The NPV distributions are not shown in this case, but it is still clear that MO does not lead to a reduced uncertainty in the achieved long-term NPV gains and offers poor uncertainty handling.

Redundant DOFs. As in the previous example, the condition to check the redundant DOFs is set to $\sigma_i/\sigma_1 < 0.02$. 52 input redundant DOFs are found, as shown in **Fig. 7.**

Results for the Switching Method. As an optimization procedure to solve for the robust version of Eq. 4, under economic uncertainty, a switching method is applied, as presented in van Essen et al. (2011). The optimal solution of the primary-objective optimization $\mathbf{u}^*_{1:K}$ serves as an initial input guess for the switching hierarchical optimization. The values of the primary and the secondary objectives are given in **Fig. 8.** Because we consider a MOO problem with contradictory objectives, for most of the iterations, the value of the primary objective decreases as the value of the secondary objective increases, and vice versa. In this example, the maximum decrease, as determined by the chosen value of ε, is equal to 0.3%. The optimization routine seems to converge after 34 iterations.

The time evolutions of NPV for all three strategies—MO, RC, and robust hierarchical optimization—are compared in **Fig. 9.** Because the secondary objective is a highly discounted NPV, we expect to see an increase in short-term gains compared with MO. With the chosen ensemble, we do not observe a plausible improvement in the short-term gains. A very small increase can be observed with hardly any decrease in the long-term gain. These results are highly dependent on the chosen ensemble of varying

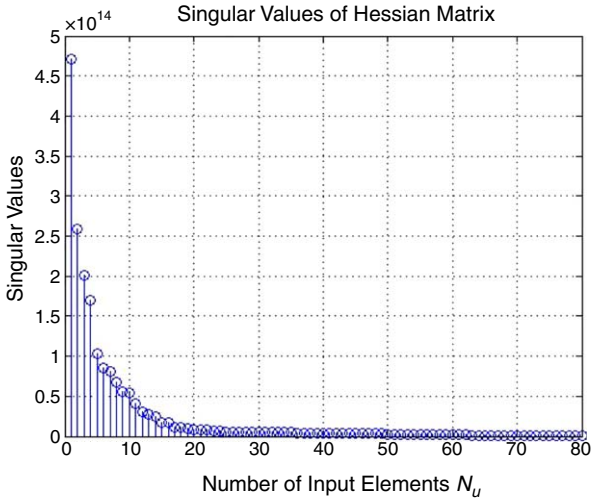

Fig. 7—Singular values of Hessian with primary objective $J_{MO,1}$ under economic uncertainty.

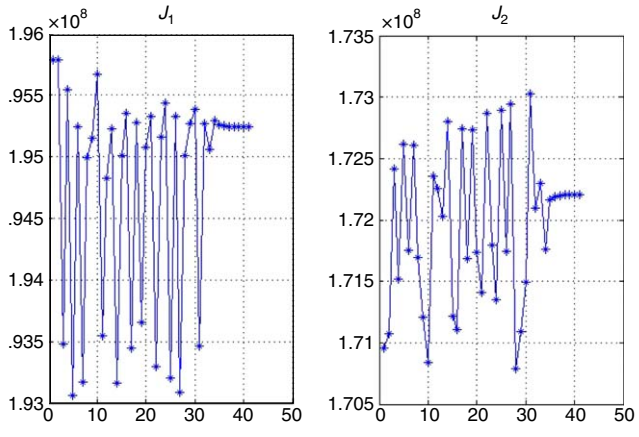

Fig. 8—Primary $J_{MO,1}$ and secondary $J_{MO,2}$ objectives with optimization-iteration numbers by use of the switching method for robust hierarchical optimization.

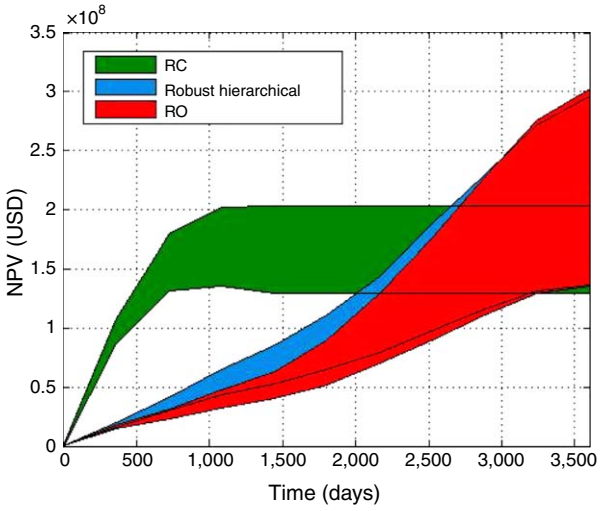

Fig. 9—Time evolutions of NPV by applying optimal inputs from MO, robust hierarchical optimization under economic uncertainty, and RC to each ensemble member.

oil prices. A different ensemble may result in a larger improvement in short-term gains.

Quantifying Effect of Uncertainty: A Robust Weighted-Sum Approach

The robust hierarchical approach provides a balance between short-term and long-term objectives. The switching method for a particular ε can be viewed as giving one point in the 2D objective-functions space determined by J_1 and J_2. From the uncertainty-handling viewpoint, it can explain how uncertainty affects both objectives for a chosen value of ε. To completely characterize and quantify the effect of uncertainty on the objective-function space while balancing both objectives, the classical weighted-sum approach is used, as will be discussed next.

Robust Weighted-Sum Approach. The weighted-sum approach can easily be extended to a robust scheme by considering the robust primary and secondary objectives, as defined previously. It takes the following form:

$$\max_{\mathbf{u}_{1:K}} \; w_1 J_{MO,1} + (1-w_1) J_{MO,2}, \quad \text{s.t. } 0 \le w_1 \le 1. \quad \ldots\ldots\ldots\ldots\ldots (9)$$

Remember that in the MO case, with geological uncertainty, $J_{MO,1}$ and $J_{MO,2}$ are given as

$$J_{MO,1} = \frac{1}{N_{\text{geo}}} \sum_{i=1}^{N_{\text{geo}}} J_1^i, \;\; J_{MO,2} = \frac{1}{N_{\text{geo}}} \sum_{i=1}^{N_{\text{geo}}} J_2^i. \quad \ldots\ldots\ldots\ldots (10)$$

The total number of N_{geo} values of J_1^i and J_2^i can be calculated with the optimal solutions obtained by solving Eq. 9 for different choices of w_1. An empirical covariance matrix $\mathbf{P}$ of $\mathbf{j}^i = [J_1^i, J_2^i]^\top$, $i = 1, 2, \cdots, N_{\text{geo}}$, is estimated for each w_1. Confidence ellipses are drawn with the help of these covariance matrices to quantify the effect of the uncertainty. Confidence ellipses can be represented as

$$(\mathbf{j} - \hat{j} \times \mathbf{1})^\top \mathbf{P}^{-1} (\mathbf{j} - \hat{j} \times \mathbf{1}) \approx \chi_\alpha^2, \quad \ldots\ldots\ldots\ldots\ldots (11)$$

where $\hat{j}$ is the mean of $\mathbf{j}$, $\mathbf{1}$ is a 2×1 vector of ones, and χ_α^2 is the chi-square distribution with α DOFs, where we have dropped the superscript i for clarity of notation. In the simulation examples, only geological uncertainty is considered for the robust weighted-sum approach. The given approach can easily be extended to consider economic uncertainties as well.

Simulation Results. The robust weighted-sum approach is implemented for different weights; i.e., $w_1 \in \{0, 0.3, 0.5, 0.7, 0.9, 1\}$. The resulting solutions are applied to the ensemble of 100 models, and in each case the J_1^i and J_2^i objectives for $i = 1, 2, 3, \ldots, 100$ are evaluated. This results in 100 points for $J_{MO,1}$ and $J_{MO,2}$ each. A 95% confidence ellipse is then used on these NPV data points to quantify the effect of uncertainty on the objective-function space for chosen values of w_1. This confidence ellipse defines the region that contains 95% of all samples that can be drawn from the preassumed Gaussian distribution of NPV points. The optimal inputs obtained from the robust weighted-sum approach and the confidence ellipse for $w_1 = 0.7$ with the 100 data points from both objectives are shown in **Figs. 10a and 10b,** respectively.

In the classical MOO framework, a Pareto-optimal curve results if none of the objective functions can be improved in value without degrading some of the other objective values. In this robust weighted-sum approach, these ellipses for different values of w_1 will form a so-called robust Pareto curve, as shown in **Fig. 11.** Because of the nonconvexity and the high complexity of the problem, it is difficult to construct a complete robust Pareto curve as in a nominal case, and it can be observed that some of the mean points are dominated by others. This robust Pareto curve is used to show the uncertainty-quantification bounds on the 2D objective-

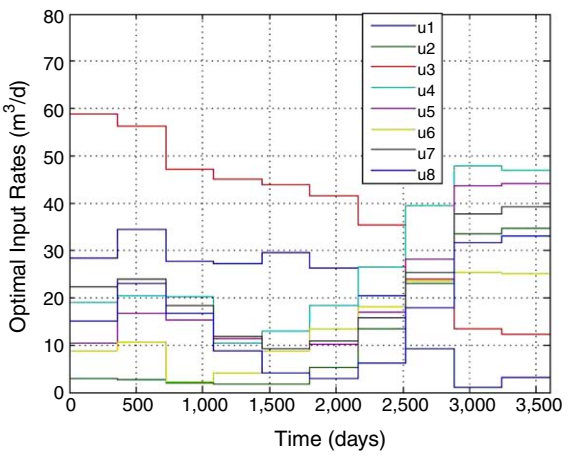

(a) Optimal injection rates

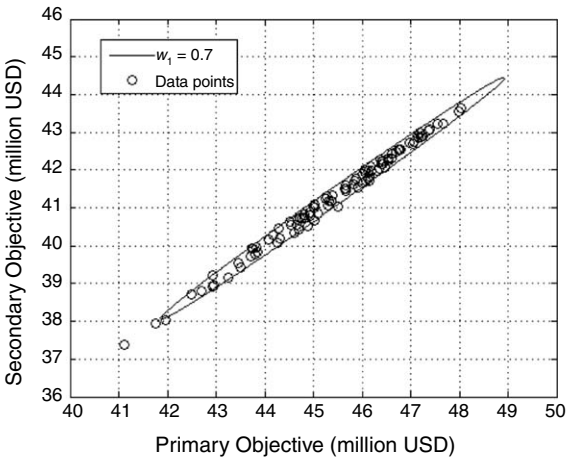

(b) The 95% confidence ellipse with 100 data points

Fig. 10—The optimal injection rates and the 95% confidence ellipse obtained from robust weighted-sum approach with $J_{MO,1}$ and $J_{MO,2}$ for w_1=0.7.

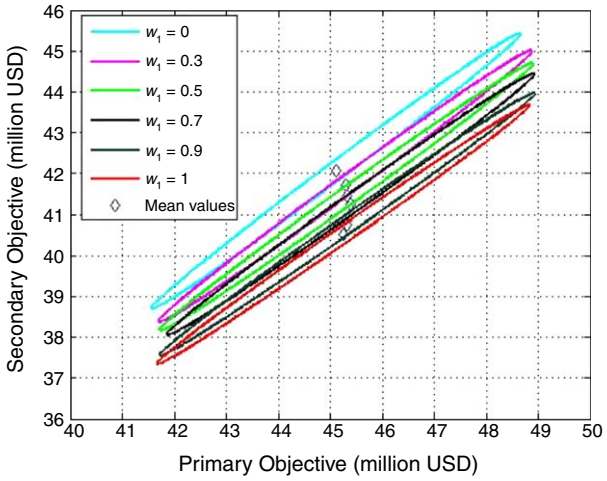

Fig. 11—The robust Pareto curve formed by the confidence ellipses for the robust weighted-sum approach by use of MO objectives for different values of w_1.

functions space, as shown in Fig. 11, and not to characterize a complete robust Pareto curve. In Liu and Reynolds (2015b), alternative algorithms—i.e., a constrained weighted-sum method and a constrained normal-boundary-intersection method by use of an augmented-Lagrange algorithm—have been proposed to develop a Pareto curve, but they have not been implemented in this work.

Fig. 12 gives the NPV time-evolution bands and the NPV distributions. As expected, the short-term gains increase with increasing weight on the secondary term; that is, with decreasing w_1. The NPV distributions show a slight compromise on long-term gains with increasing short-term values. Hence, the robust weighted-sum approach also provides a balance between short-term and long-term objectives. With different weights, the desired level of balance can be achieved.

These robust MO schemes (i.e., the robust hierarchical and robust weighted-sum approaches), with the averaging objectives, incorporate uncertainty in the optimization framework. However, they do not aim at reducing the effect of uncertainty in the resulting NPV, such as by reducing the width (variance) of the NPV distribution. MO is a so-called risk-neutral objective. A larger uncertainty will result in a bigger spread (or variance) of the NPV distribution, and vice versa. From an economic perspective, this seriously limits the performance of MO to handle uncertainty, as well as the performance of the proposed robust MOO approaches. In the next section, a risk-averse mean-variance objective is presented.

The MVO Approach

Introduction. Markowitz (1952) has introduced a risk-return portfolio-selection approach, where a "return" is maximized while minimizing the "risk" associated with it. It has introduced a quantitative characterization of risk in terms of the variance of the returns. On the basis of the investor's attitude toward risk, a risk-return profile is selected. Various ways have been introduced to characterize risk, such as percentile-based risk measures like value at risk and conditional value at risk (Rockafellar 2007; Yasari et al. 2013, Capolei et al. 2015a; Siraj et al. 2015c). In this work, the return is considered as the average NPV, whereas the risk is characterized with the spread or the variance of the NPV distribution. MVO enables a reduction of the variance of the NPV distribution, which results in a reduction of the sensitivity of the optimal solution to uncertainties; that is, it minimizes the negative effect of uncertainty. The mean-variance objective function J_{MVO} for an ensemble of N_{geo} models can be defined as

$$J_{MVO} = J_{MO} - \gamma J_V, \quad \ldots\ldots\ldots\ldots\ldots\ldots\ldots\ldots\ldots\ldots (12)$$

where J_{MO} and J_V are the mean NPV and the variance of NPV, respectively, and γ is the weighting on the variance term. Because mean and variance have different dimensions, γ plays a dual role as scaling factor. J_{MO} is the same as given in Eq. 5 whereas the variance of the NPV is given as

$$J_V = \frac{1}{N_{\text{geo}} - 1} \sum_{i=1}^{N_{\text{geo}}} (J_i - J_{MO})^2. \quad \ldots\ldots\ldots\ldots\ldots\ldots\ldots (13)$$

This approach can be extended to consider economic uncertainty by replacing averaging over the ensemble of N_{geo} model realizations to the ensemble of N_{eco} oil-price scenarios.

The MO objective in the robust weighted-sum approach is replaced by the MVO objective for better uncertainty handling. The details of this scheme are given later in this paper. The results for both MO and MVO objectives in the robust-weighted-sum approach are also compared.

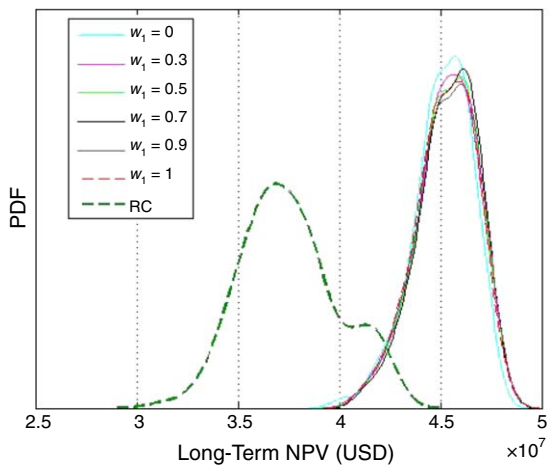

(a) PDF (long-term NPV) by applying optimal inputs from robust weighted-sum using MO objectives for different w_1 and RC to each ensemble member

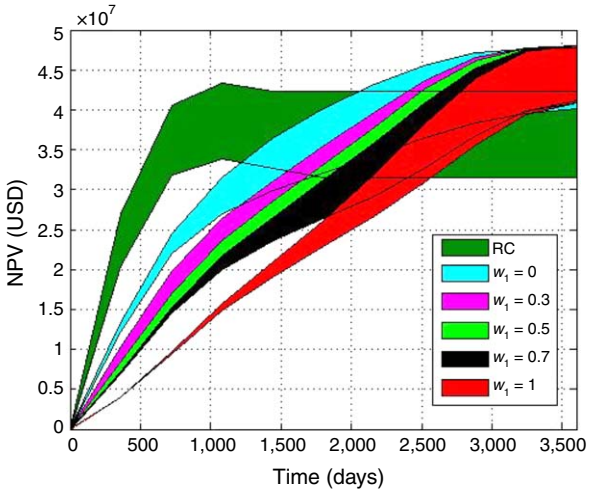

(b) Maximum and minimum (band) for time evolutions of NPV by applying optimal inputs from robust weighted-sum using MO objectives for different w_1 and RC to each ensemble member

Fig. 12—Results comparison in terms of long-term and time evolutions of NPV for the robust weighted-sum approach by use of MO objectives for different w_1 and RC.

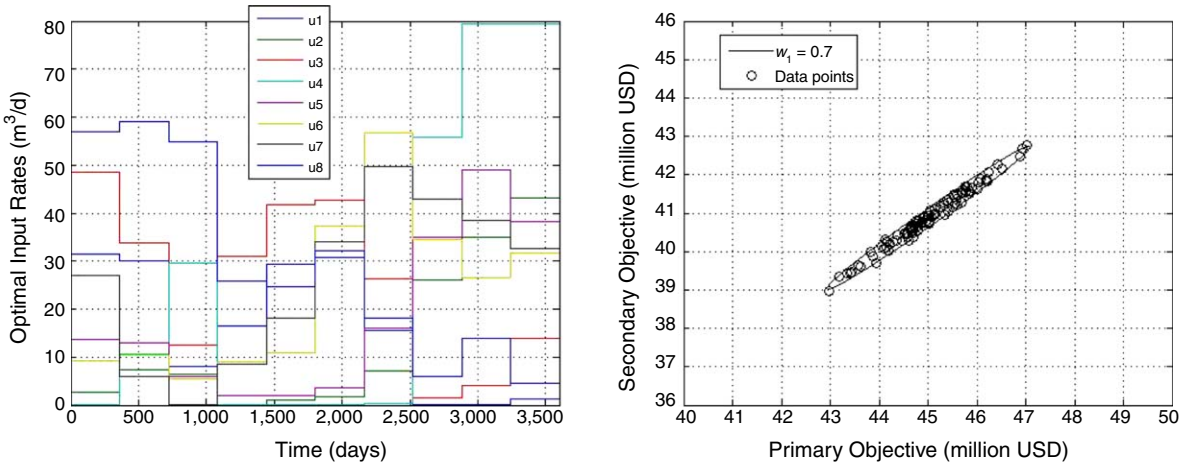

(a) Optimal injection rates

(b) The 95% confidence ellipse with 100 data points

Fig. 13—The optimal injection rates and the 95% confidence ellipse obtained from the robust weighted-sum approach with $J_{MVO,1}$ and $J_{MVO,2}$ for $w_1=0.7$.

Robust Weighted-Sum Approach With MVO Under Geological Uncertainty. By replacing the objectives in Eq. 9 by the MVOs for the geological uncertainty, the robust weighted-sum approach can be written as

$$\max_{\mathbf{u}_{1:K}} \; w_1 J_{MVO,1} + (1-w_1) J_{MVO,2}, \quad \text{s.t. } 0 \le w_1 \le 1, \quad \ldots\ldots\ldots\ldots\ldots (14)$$

where J_{MVO} is the MVO, as defined in Eq. 12. $J_{MVO,1}$ represents the undiscounted primary (long-term) MVO and $J_{MVO,2}$ is the highly discounted secondary (short-term) MVO.

Results of the Robust Weighted-Sum Approach With MVO. The proposed approach is implemented for a fixed value of γ; i.e., $\gamma = 2 \times 10^{-6}$. The weights are chosen as $w_1 \in \{0, 0.3, 0.5, 0.7, 0.9, 1\}$. The resulting solutions are applied to the ensemble of 100 models, and in each case both J_1^i and J_2^i objectives for $i = 1, 2, 3, \ldots, 100$ are evaluated. This results in 100 points for $J_{MVO,1}$ and $J_{MVO,2}$ each. A 95% confidence ellipse is then used on these data points to quantify the effect of uncertainty on the objectives. The optimal inputs obtained from the robust weighted-sum approach and the confidence ellipse for $w_1 = 0.7$ with the data points for both objectives are shown in **Figs. 13a and 10b,** respectively.

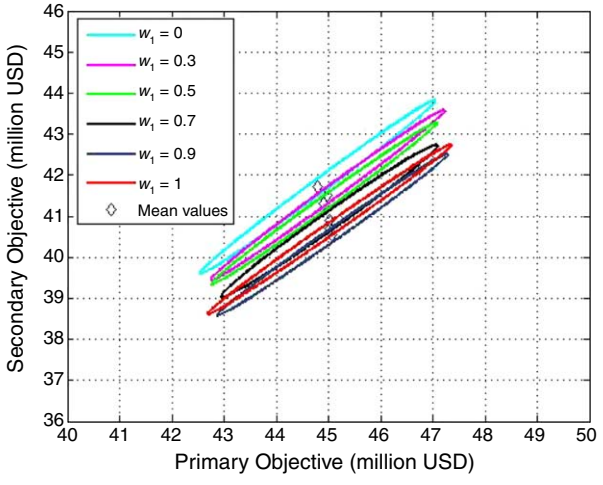

Fig. 14—The robust Pareto curve formed by the confidence ellipses from the robust weighted-sum approach by use of the MVO objectives for different values of w_1.

Similar to the previous case, the confidence ellipses for each w_1 in Eq. 14 form a robust Pareto curve, as shown in **Fig. 14,** with the mean value of each ellipse indicated by diamonds.

For the sake of comparison with MO, the Fig. 14 axes scales are chosen to be the same. It can easily be seen that because of the reduction of variance, these ellipses are small compared with those for the MO objective, as shown in Fig. 11. Hence, in this example, the robust weighted-sum approach with MVO reduces the negative effect of uncertainty and provides better uncertainty handling. **Fig. 15** gives the NPV time-evolution bands and the NPV distributions. As expected, the short-term gains increase with increasing weight on the secondary objective; that is, with decreasing w_1. The NPV distributions show a very-slight compromise on long-term gains with increasing short-term values.

A comparison between the two approaches is made by comparing the areas of all ellipses resulting from each w_1. The area can be calculated as

$$A = 5.991\pi ab, \quad \ldots\ldots\ldots\ldots\ldots\ldots\ldots\ldots\ldots\ldots (15)$$

where a and b are the major and the minor axis of the ellipse, and the factor 5.991 corresponds to a 95% confidence interval. It can be seen in **Fig. 16** that because of the better handling of uncertainty by MVO, the ellipses corresponding to MVO have a smaller area compared with those corresponding to MO.

The results of the robust weighted-sum approach show the better uncertainty handling of the MVO approach. In the next section, a single-objective MVO is formulated. It is investigated whether by explicit handling of uncertainty in model-based economic optimization, the balance between short-term and long-term gains can be naturally obtained. Economic uncertainty is explicitly considered together with geological uncertainty.

MVO as a Single Objective

The single-objective MVO approach, as discussed previously, is implemented with the same ensemble of model realizations, economic data, and control inputs (with 20 control time intervals). First, we focus on the geological uncertainty. An undiscounted NPV is used. Different values of γ—$\gamma \in [1 \times 10^{-6}, 3 \times 10^{-6}, 7 \times 10^{-6}]$—are used. The obtained MVO optimal strategies are applied to each member of the geological ensemble, resulting in 100 NPV values for each γ. The corresponding PDFs of these NPV values and the PDFs obtained from the MO and the RC approaches are shown in **Fig. 17a.** Nominal strategies are not compared for the sake of clarity. The first observation is that the variance is reduced with increasing γ; the higher the value of γ, the lower the variance. The lower variance is achieved at the cost of compromising the average NPV. Because the effect of

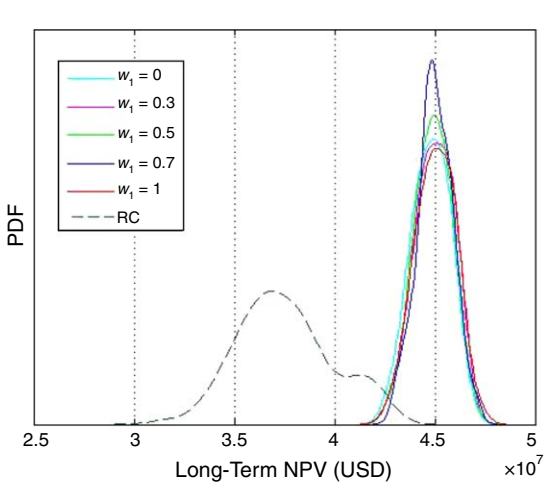

(a) PDF (long-term NPV) by applying optimal inputs from robust weighted-sum using MVO objectives for different w_1 and RC to each ensemble member

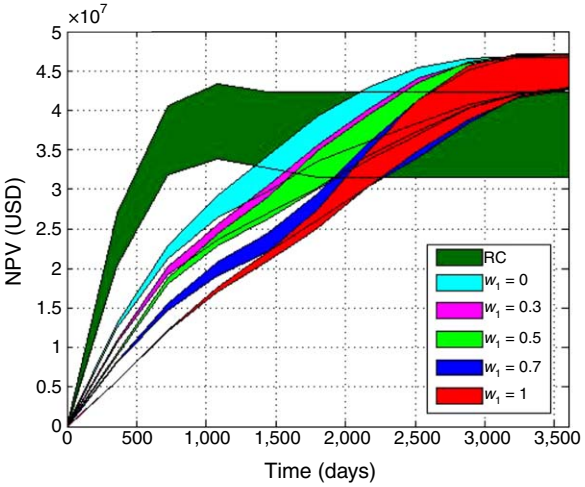

(b) Maximum and minimum (band) for time evolutions of NPV by applying optimal inputs from robust weighted-sum using MVO objectives for different w_1 and RC to each ensemble member

Fig. 15—Results comparison in terms of long-term and time evolutions of NPV for the robust weighted-sum approach with MVO objectives.

uncertainty is visible by the spread of the NPV distribution, the reduction of the variance reflects the reduction in sensitivity of the strategy to uncertainty. Hence, MVO aims to mitigate the negative effect of the uncertainty on the NPV distribution.

The time evolutions of NPV for all three strategies, MVO, MO, and RC, are compared in Fig. 17b. It can be observed that, compared with the MO strategy, all MVO strategies provide a faster buildup of NPV over time (high short-term gains) at the cost of slightly compromising the long-term gains. It can also be observed that the value of γ affects the rate of NPV buildup with a respective reduction of the average long-term gain. In portfolio optimization, the selection of γ provides a way to choose a risk-return profile as per the investors' interest. But in this example, it also plays a role of an explicit parameter to balance short-term and long-term economic objectives according to the investors' choice.

The results show that the single-objective MVO naturally provides higher short-term gains without (artificially) changing the economic criteria; i.e., NPV with high discount factor, as in the robust MOO schemes. For clarity in representing results, the average values for the time evolutions of NPV bands for all three strategies are compared in **Fig. 18.**

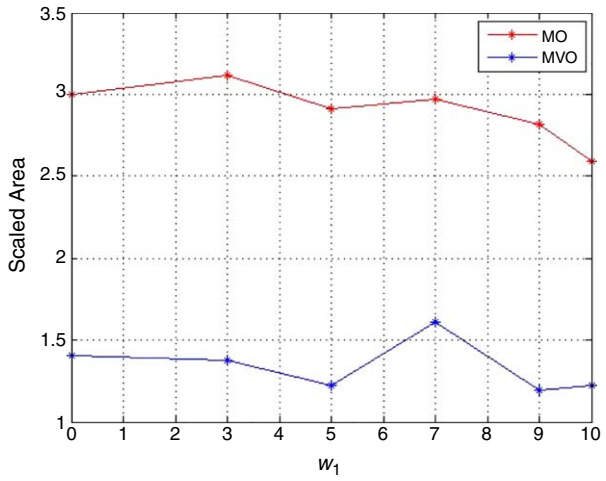

Fig. 16—Comparison of robust weighted-sum approaches by use of MO and MVO objectives in terms of area of ellipses for each w_1.

The numerical results of the behavior of average NPV are summarized in **Table 1.** Table 1 shows the average NPV obtained for all the control strategies at 720 days of oil production and the average NPV obtained at the end of the simulation period, which was 3,600 days. An increase of the average NPV at Day 720 and a decrease at the end of the simulation period compared with the MO are shown. The first observation is that the MO has the lowest average NPV at Day 720, whereas it results in the maximum average NPV at the end of the simulation period compared with other strategies. RC has a maximum increase in the short-term gains but with a decrease of 6.31% compared with the MO. For the MVO strategies, as discussed previously, γ provides an explicit way of balancing the short-term and the long-term objectives and hence becomes a tuning parameter for balancing both objectives. A higher value of γ will result in a faster buildup of NPV at the cost of compromising the final NPV.

As the simulation with robust hierarchical optimization with geological uncertainty runs into numerical problems with 20 control steps, a different step size of 10 is used. The results are slightly different for MO and RC with 10 control steps and compared with the robust hierarchical optimization in **Table 2.** The robust hierarchical approach outperforms all MVO strategies because of higher short-term gains of 119%, with almost no decrease from MO at the end of the life cycle. One of the major advantages of the robust hierarchical optimization approach is the ability to allow a predetermined maximal decrease, indicated by ε, on the primary objective to improve the secondary objective.

Results for MVO With Economic Uncertainty. In this case, we only consider economic uncertainty and a single realization of the standard egg model is used. The MVO with economic uncertainty is implemented with 10 different oil-price scenarios, as shown in Fig. 5. Different values of γ—i.e., $\gamma \in [1 \times 10^{-7},\ 2 \times 10^{-7},\ 3 \times 10^{-7}]$—are used. The MO and RC strategies are applied to the single-model realization with each oil-price realization resulting in 10 different NPVs. The time evolutions of NPV for these strategies are compared in **Fig. 19b.** The widths of the bands clearly show that the economic uncertainty (i.e., varying oil prices) have a very profound effect on the obtained NPV. The large uncertainty in the oil-price scenarios is mapped to a large spread of the NPV bands. All three MVO strategies, $\gamma \in [1 \times 10^{-7},\ 2 \times 10^{-7},\ 3 \times 10^{-7}]$, are also applied to the

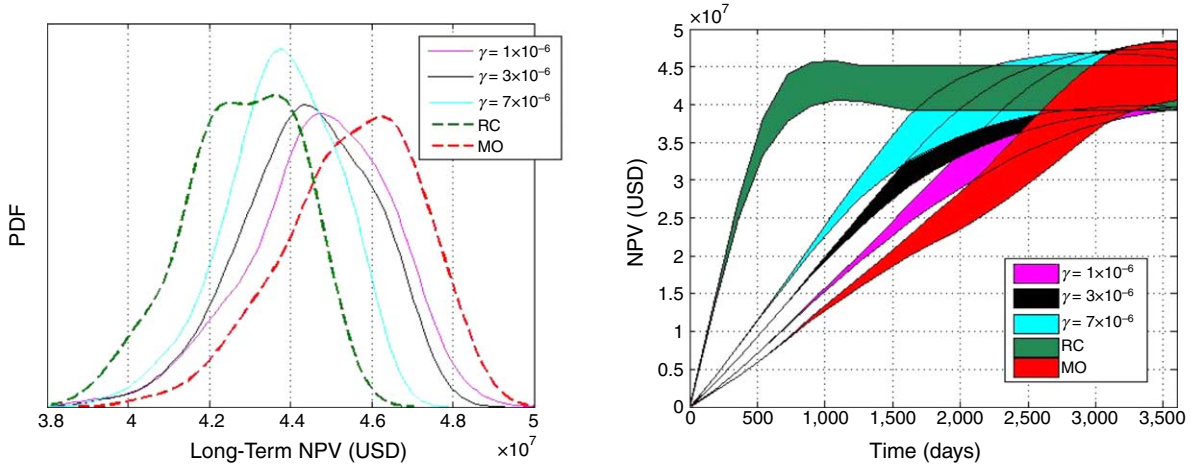

(a) PDF (long-term NPV) by applying optimal inputs from MO and MVO under geological uncertainty and RC to each ensemble member

(b) Maximum and minimum (band) for time evolutions of NPV by applying optimal inputs from MO and MVO under geological uncertainty and RC to each ensemble member

Fig. 17—Results comparison in terms of long-term NPV and time evolution of NPV for single-objective MVO, MO under geological uncertainty, and RC.

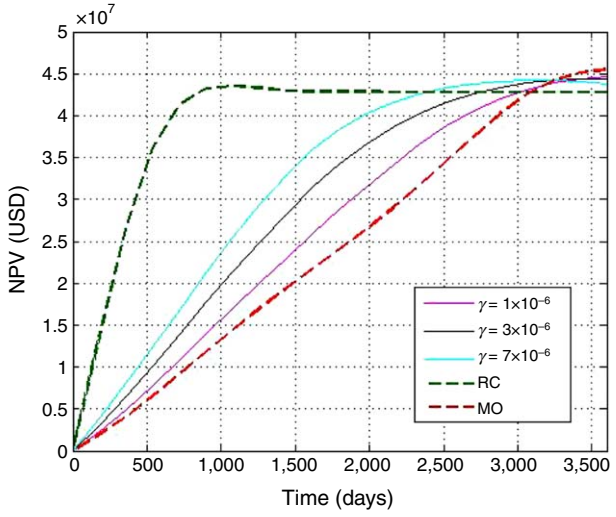

Fig. 18—Average values for the time evolutions (bands) of NPV by applying optimal inputs from MO and MVO under geological uncertainty and RC to each ensemble member.

single-model realizations with 10 different oil-price realizations. It results in three different bands for each MVO strategy, but for the sake of clarity, only one time-evolutions band of NPV for $\gamma = 1 \times 10^{-7}$ is shown in Fig. 19b.

Fig. 19a shows the average NPV values of the bands. The results for the MVO strategies for three different values of γ are also shown in Fig. 19a. With MVO approaches, an improvement in the short-term gains compared with the MO case can be observed. Similar to the case of geological uncertainty, γ becomes an explicit parameter to balance short-term and long-term gains.

The numerical results are summarized in **Table 3.** Similar to Table 1, Table 3 shows the average NPV obtained for all the control strategies at 720 days of oil production and the average NPV obtained at the end of the simulation period of the reservoir model (3,600 days), with percentage increase and decrease compared with the MO. As with the geological uncertainty, the MO has a lowest average NPV at Day 720 with a maximum average NPV at the end of the simulation period compared with the other strategies. RC has a maximum increase in the short-term gains, but with a decrease of 17.6% compared with the MO; RC reaches its maximum NPV, 161.2 million USD, after approximately 2 years of production. Economic uncertainty has a profound effect on NPV optimization compared with the geological uncertainty; with the MVO strategy with $\gamma = 3 \times 10^{-8}$, an increase of 318.5% on

Control Strategies	Average NPV at Day 720	Increase From MO (%)	Average NPV at Day 3,600	Decrease From MO (%)
MO	9.2 million USD	–	45.5 million USD	–
$\gamma = 1\times10^{-6}$	10.8 million USD	18.4%	44.7 million USD	1.71%
$\gamma = 3\times10^{-6}$	13.9 million USD	51.9%	44.4 million USD	2.42%
$\gamma = 7\times10^{-6}$	16.9 million USD	84.4%	43.7 million USD	3.78%
RC	41.3 million USD	350%	42.8 million USD	6.31%

Table 1—Results for geological uncertainty (single-objective MVO).

Control Strategies	Average NPV at Day 720	Increase From MO (%)	Average NPV at Day 3,600	Decrease From MO (%)
MO	9.9 million USD	–	45.3 million USD	–
Robust hierarchical	21.7 million USD	119%	45.3 million USD	0%
RC	36.1 million USD	264%	38.6 million USD	14.7%

Table 2—Results for geological uncertainty (robust hierarchical optimization).

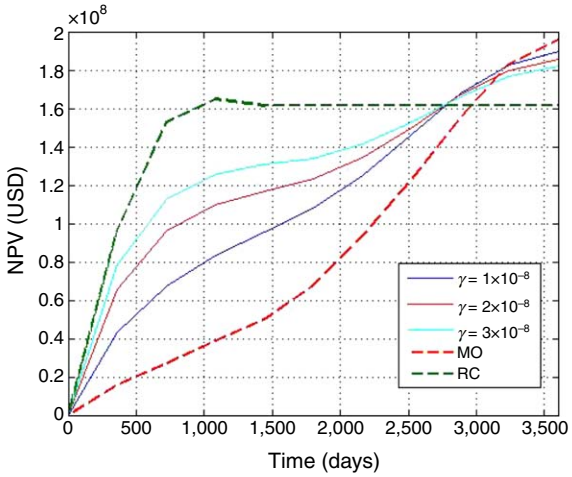

(a) Average values for the time evolutions (bands) of NPV by applying optimal inputs from MO and MVO under economic uncertainty and RC to each ensemble member

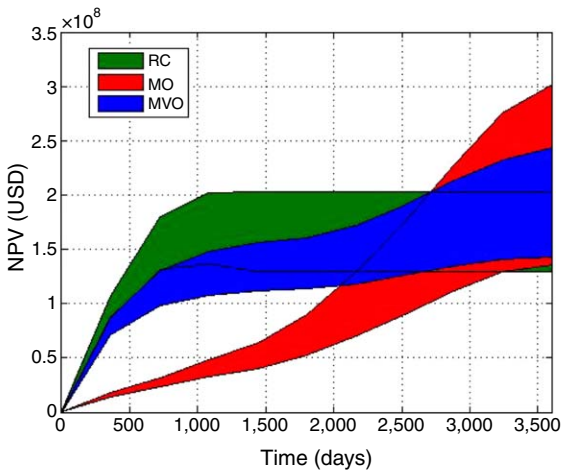

(b) Maximum and minimum (band) for time evolutions of NPV by applying optimal inputs from MO and MVO under economic uncertainty and RC to each ensemble member

Fig. 19—Results comparison for single-objective MVO, MO under economic uncertainty, and RC.

short-term gains can be achieved at the cost of a 7.1% decrease on final NPV, compared with an RC strategy with an increase of 467.6% on the short-term and with a significant drop of 17.6% on long-term gains. Here again, γ provides an explicit way of balancing short-term and long-term objectives and hence provides decision makers a tuning parameter for balancing both objectives. The robust hierarchical multiobjective approach provides an improvement in short-term gains by 30.85% at the cost of reducing long-term gains with 0.3%.

Conclusions

Model-based NPV optimization suffers from high levels of uncertainty and also typically results in low short-term gains. It is desirable to explicitly include uncertainty, and hence add robustness to the predicted long-term NPV, while also offering a good balance between the short-term and long-term gains. From this work, the following conclusions can be drawn.

1. The question of how to obtain a robust solution that also provides a good balance of short- and long-term objectives is addressed by use of MOO approaches. It has been shown by simulation examples that because of the availability of redundant DOFs in robust optimization, the short-term gains can be greatly improved without compromising long-term gains. In the situation of geological uncertainty, a plausible increase is observed, whereas for the case of economic uncertainty, the improvement is less than expected. These results may vary with different characterizations of uncertainty (with different ensembles).
2. The classic weighted-sum approach is extended to a robust setting by including robust MO objectives. It has been shown that MO does not reduce the effect of uncertainty on the achieved NPV and thus provides poor uncertainty handling. Therefore, a risk-return strategy with an MVO is considered. The weighted-sum approach is implemented with the MVO objectives, and a reduced effect of uncertainty compared with MO is obtained.
3. It has been shown that a robust MVO approach, although not specifically focused on short-term gains, has a natural effect of increasing the short-term gains. This effect has been shown to be more dominant in the situation of economic uncertainty than in the case of geological uncertainty.

Nomenclature

A = area of confidence ellipses
b = discount factor
$\mathbf{g}$ = nonlinear reservoir-model dynamics
h = perturbation-step size
$\mathbf{h}$ = nonlinear reservoir-output function
H = Hessian matrix
J = NPV objective
J_{MO} = MO NPV
$J_{MO,1}$ = undiscounted primary (long-term) MO
$J_{MO,2}$ = highly discounted secondary (short-term) MO
J_{MVO} = MVO objective
$J_{MVO,1}$ = undiscounted primary (long-term) MVO
$J_{MVO,2}$ = highly discounted secondary (short-term) MVO
J_V = variance of NPV objective
k = discrete instants of time
K = total number of timesteps
N_{eco} = number of oil-price realizations in an ensemble
N_{geo} = number of model realizations in an ensemble
N_u = number of input elements
$\mathbf{P}$ = empirical covariance matrix
$q_{\text{inj},k}$ = total flow rate of injected water
$q_{o,k}$ = total flow rate of produced oil
$q_{w,k}$ = total flow rate of produced water
r_{inj} = water-injection cost

Control Strategies	Average NPV at Day 720	Increase From MO (%)	Average NPV at Day 3,600	Decrease From MO (%)
MO	26.9 million USD	–	196 million USD	–
$\gamma = 1\times10^{-8}$	67.6 million USD	151%	190 million USD	3.0%
$\gamma = 2\times10^{-8}$	96.2 million USD	257%	185 million USD	5.1%
$\gamma = 3\times10^{-8}$	112 million USD	318%	181 million USD	7.1%
Robust hierarchical	35.2 million USD	30.8%	195 million USD	0.3%
RC	152 million USD	467%	161 million USD	17.6%

Table 3—Results for economic uncertainty.

r_o = oil price
r_w = water-production cost
$\mathbf{u}$ = control vector
w_i = weighting scalars in robust weighted-sum approach
$\mathbf{x}$ = state variables
$\mathbf{y}$ = measured output variables
γ = weighting on the variance term in MVO objective
Δt_k = time interval of timestep k
$\boldsymbol{\theta}$ = parameter vector
τ_t = reference time for discount factor b
χ^2_α = chi-square distribution with α DOFs

Acknowledgments

The authors acknowledge financial support from the Recovery Factory program sponsored by Shell Global Solutions International.

References

Aziz, K. and Settari, A. 1979. *Petroleum Reservoir Simulation*. London. Applied Science Publishers.

Bhattacharyya, S. C. and Timilsina, G. R. 2010. A Review of Energy System Models. *Int. J. Energ. Sec. Mgmt.* **4** (4): 494–518. https://doi.org/10.1108/17506221011092742.

Birol, F. 2010. *World Energy Outlook 2010*. Paris: International Energy Agency.

Brouwer, D. R. and Jansen, J. D. 2004. Dynamic Optimization of Waterflooding With Smart Wells Using Optimal Control Theory. *SPE J.* **9** (4): 391–402. SPE-78278-PA. https://doi.org/10.2118/78278-PA.

Capolei, A., Foss, B., and Jorgensen, J. B. 2015a. Profit and Risk Measures in Oil Production Optimization. *Proc*., 2nd IFAC Workshop on Automatic Control in Offshore Oil and Gas Production, Florianópolis, Brazil, 27–29 May, Vol. 48, Issue 6, 214–220. https://doi.org/10.1016/j.ifacol.2015.08.034.

Capolei, A., Suwartadi, E., Foss, B. et al. 2015b. A Mean–Variance Objective for Robust Production Optimization in Uncertain Geological Scenarios. *J. Pet. Sci. Eng.* **125** (January): 23–37. https://doi.org/10.1016/j.petrol.2014.11.015.

Chen, C., Li, G., Reynolds, A. et al. 2012. Robust Constrained Optimization of Short- and Long-Term Net Present Value for Closed-Loop Reservoir Management. *SPE J.* **17** (3): 849–864. SPE-141314-PA. https://doi.org/10.2118/141314-PA.

Chen, Y. and Oliver, D. S. 2010. Ensemble-Based Closed-Loop Optimization Applied to Brugge Field. *SPE J.* **13** (1): 56–71. SPE-118926-PA. https://doi.org/10.2118/118926-PA.

Chen, C., Wang, Y., Li, G. et al. 2010. Closed-Loop Reservoir Management on the Brugge Test Case. *Computational Geosciences* **14** (4): 691–703. https://doi.org/10.1007/s10596-010-9181-7.

Criqui, P. 2001. POLES: Prospective Outlook on Long-Term Energy Systems. Information document, LEPII-EPE, Grenoble, France, http://web.upmfgrenoble.fr/lepiiepe/textes/POLES8p_01.pdf (accessed 18 January 2017).

Fonseca, R. M., Stordal, A. S., Leeuwenburgh, O. et al. 2014. Robust Ensemble-Based Multi-Objective Optimization. *Proc.,* ECMOR XIV: 14th European Conference on Mathematics in Oil Recovery, Catania, Italy, 8–11 September. https://doi.org/10.3997/2214-4609.20141895.

Foss, B. 2012. Process Control in Conventional Oil and Gas Fields–Challenges and Opportunities. *Control. Eng. Pract.* **20** (10): 1058–1064. https://doi.org/10.1016/j.conengprac.2011.11.009.

Haimes, Y. Y. and Li, D. 1988. Hierarchical Multiobjective Analysis for Large-Scale Systems: Review and Current Status. *Automatica* **24** (1): 53–69. https://doi.org/10.1016/0005-1098(88)90007-6.

Jansen, J. D. 2011. Adjoint-Based Optimization of Multi-Phase Flow Through Porous Media–A Review. *Comput. Fluid.* **46** (1): 40–51. https://doi.org/10.1016/j.compfluid.2010.09.039.

Jansen, J. D., Bosgra, O. H., and Van den Hof, P. M. J. 2008. Model-Based Control of Multiphase Flow in Subsurface Oil Reservoirs. *J. Process Contr.* **18** (9): 846–855. https://doi.org/10.1016/j.jprocont.2008.06.011.

Jansen, J. D., Fonseca, R. M., Kahrobaei, S. et al. 2014. The Egg Model–A Geological Ensemble for Reservoir Simulation. *Geosci. Dat. J.* **1** (2): 192–195. https://doi.org/10.1002/gdj3.21.

Lapillonne, B., Chateau, B., Criqui, P. et al. 2007. World Energy Technology Outlook: 2050–WETO-H_2. Brussels, Belgium: European Commission.

Lie, K.-A., Krogstad, S., Ligaarden, I. S. et al. 2012. Open-Source MATLAB Implementation of Consistent Discretisations on Complex Grids. *Computat. Geosci.* **16** (2): 297–322. https://doi.org/10.1007/s10596-011-9244-4.

Liu, X. and Reynolds, A. C. 2015a. Multiobjective Optimization for Maximizing Expectation and Minimizing Uncertainty or Risk with Application to Optimal Well Control. Presented at the SPE Reservoir Simulation Symposium, Houston, 23–25 February. SPE-173216-MS. https://doi.org/10.2118/173216-MS.

Liu, X. and Reynolds, A. C. 2015b. Pareto Optimal Solutions for Minimizing Risk and Maximizing Expected Value of Life-Cycle NPV of Production under Nonlinear Constraints. Presented at the SPE Reservoir Simulation Symposium, Houston, 23–25 February. SPE-173274-MS. https://doi.org/10.2118/173274-MS.

Ljung, L. 1999. *System Identification–Theory for the User*. Upper Saddle River, New Jersey: Prentice Hall.

Markowitz, H. 1952. Portfolio Selection. *J. Financ.* **7** (1): 77–91. https://doi.org/10.1111/j.1540-6261.1952.tb01525.x.

Nocedal, J. and Wright, S. 2006. *Numerical Optimization*. New York City: Springer Science & Business Media.

Rockafellar, R. T. 2007. Coherent Approaches to Risk in Optimization Under Uncertainty. In *INFORMS Tutorials in Operations Research: OR Tools and Applications—Glimpses of Future Technologies*, ed. P. Gray, Chap. 3, 38–61. Catonsville, Maryland: INFORMS. https://doi.org/10.1287/educ.1073.0032.

Sarma, P., Aziz, K., and Durlofsky, L. J. 2005. Implementation of Adjoint Solution for Optimal Control of Smart Wells. Presented at the SPE Reservoir Simulation Symposium, The Woodlands, Texas, 31 January–2 February. SPE-92864-MS. https://doi.org/10.2118/92864-MS.

Siraj, M. M., Van den Hof, P. M. J., and Jansen, J. D. 2015a. Model and Economic Uncertainties in Balancing Short-Term and Long-Term Objectives in Water-Flooding Optimization. Presented at the SPE Reservoir Simulation Symposium, Houston, 23–25 February. SPE-173285-MS. https://doi.org/10.2118/173285-MS.

Siraj, M. M., Van den Hof, P. M. J., and Jansen, J. D. 2015b. Handling Risk of Uncertainty in Model-Based Production Optimization: A Robust Hierarchical Approach. *Proc.,* 2nd IFAC Workshop on Automatic Control in Offshore Oil and Gas Production, Florianópolis, Brazil, 27–29 May, Vol. 48, Issue 6, 248–253. https://doi.org/10.1016/j.ifacol.2015.08.039.

Siraj, M. M., Van den Hof, P. M. J., and Jansen, J. D. 2015c. Risk Management in Oil Reservoir Waterflooding Under Economic Uncertainty. *Proc.,* 54th IEEE Conference on Decision and Control, Osaka, Japan, 15–18 December, 7542–7547. https://doi.org/10.1109/CDC.2015.7403410.

Strang, G. 2011. *Introduction to Linear Algebra*. Wellesley, Massachusetts: Wellesley-Cambridge Press.

Van den Hof, P. M. J., Jansen, J. D., and Heemink, A. 2012. Recent Developments in Model-Based Optimization and Control of Subsurface Flow in Oil Reservoirs. *Proc.,* 1st IFAC Workshop on Automatic Control in Offshore Oil and Gas Production, Trondheim, Norway, Vol. 45, Issue 8, 189–200. https://doi.org/10.3182/20120531-2-NO-4020.00047.

van Essen, G., Van den Hof, P. M. J., and Jansen, J. D. 2011. Hierarchical Long-Term and Short-Term Production Optimization. *SPE J.* **16** (1): 191–199. SPE-124332-PA. https://doi.org/10.2118/124332-PA.

van Essen, G., Zandvliet, M., Van den Hof, P. M. J. et al. 2009. Robust Waterflooding Optimization of Multiple Geological Scenarios. *SPE J.* **14** (1): 202–210. SPE-102913-PA. https://doi.org/10.2118/102913-PA.

Yasari, E., Pishvaie, M. R., Khorasheh, F. et al. 2013. Application of Multi-Criterion Robust Optimization in Waterflooding of Oil Reservoir. *J. Pet. Sci. Eng.* **109** (September): 1–11. https://doi.org/10.1016/j.petrol.2013.07.008.

Yeten, B., Durlofsky, L. J., and Aziz, K. 2003. Optimization of Nonconventional Well Type, Location, and Trajectory. *SPE J.* **8** (3): 200–210. SPE-86880-PA. https://doi.org/10.2118/86880-PA.

M. Mohsin Siraj is a post-doctoral-degree researcher at the Department of Electrical Engineering, Eindhoven University of Technology, The Netherlands. Previously, he was a PhD

degree student in the same department. Siraj's current research interests include model-based control and optimization under uncertainty, robust optimization, risk management, and data analytics (data-driven identification for dynamical systems). He holds a bachelor's degree in electronics engineering from Mehran University of Engineering and Technology, Pakistan, and a master's degree in systems and control from Eindhoven University of Technology.

Paul Van den Hof is a professor of control systems in the Department of Electrical Engineering at Eindhoven University of Technology. His current research interests are in system identification and model-based control and optimization, with applications in several technology domains, including petroleum-reservoir-engineering systems. Van den Hof holds master's and PhD degrees from Eindhoven University of Technology.

Jan-Dirk Jansen is a professor of reservoir systems and control and head of the Department of Geoscience and Engineering at Delft University of Technology, The Netherlands. Previously, he worked for Shell International in research and operations. Jansen's current research interests are the use of systems and control theory for production optimization and reservoir management. He holds master's and PhD degrees from Delft University of Technology.